Application of Proteomic Profiling Based on 2D-DIGE for Classification of Compounds According to the Mechanism of Action

Makoto Muroi,[1] Sayaka Kazami,[1,2] Kazue Noda,[1] Hisae Kondo,[1] Hiroshi Takayama,[1,2] Makoto Kawatani,[1] Takeo Usui,[3] and Hiroyuki Osada[1,2,*]

[1]Chemical Library Validation Team, Chemical Biology Core Facility, Chemical Biology Department, RIKEN Advanced Science Institute,
2-1 Hirosawa, Wako-shi, Saitama 351-0198, Japan
[2]Graduate School of Science and Engineering, Saitama University, 255 Shimo-Okubo, Saitama 338-8570, Japan
[3]Graduate School of Life and Environmental Sciences, University of Tsukuba, Tsukuba, Ibaraki 305-8572, Japan
*Correspondence: hisyo@riken.jp

SUMMARY

The development of new anticancer agents derived from natural resources requires a rapid identification of their molecular mechanism of action. To make this step short, we have initiated the proteomic profiling of HeLa cells treated with anticancer drugs representing a wide spectrum of mechanisms of action using two-dimensional difference gel electrophoresis (2D-DIGE). Unique proteome patterns were observed in HeLa cells treated with the HSP90 inhibitor geldanamycin, and were similar to the patterns induced by radicicol, a structurally different HSP90 inhibitor. On the other hand, etoposide and ICRF-193, compounds claimed to be topoisomerase II inhibitors, showed different proteomic profiles, which reflect their different biological activities as revealed by cell-cycle analysis. Thus far, combined data from 19 compounds have allowed their successful classification by cluster analysis according to the mechanism of action.

INTRODUCTION

Cell-based assays are widely used in drug discovery because the assessment of molecular interaction occurs within the context of a living cellular environment (Baker et al., 2007). Many bioactive compounds inhibiting the growth of cancer cells have been isolated using a cell-based screen (Kakeya et al., 2002; Kawada et al., 2009). In most instances, the molecular target for newly isolated compounds remains unknown. The identification of a plausible target is sometimes possible based on the results of cell-based assays; however, the exact target must be proven by enzymatic assays, analyses of binding proteins, or genetic methods employing an siRNA (Kazami et al., 2006; Sato et al., 2007; Teruya et al., 2005). The confirmation of molecular targets, however, is usually a difficult and time-consuming process.

Multidimensional phenotype profiling approaches have a capacity to generate a testable hypothesis related to the mechanism of action and eventual off-target effects of new compounds. The differential sensitivity of the panel of cancer cell lines to the compounds has been used to identify their molecular target(s). The most commonly used assay, the NCI 60 antitumor screen, allowed the identification of benzolactone enamide as an inhibitor of V-ATPase (Boyd et al., 2001). Another panel consisting of 39 different cancer cell lines identified the compound encoded as ZSTK474 to be an inhibitor of phosphatidylinositol 3-kinase (Yaguchi et al., 2006). Recent advances in the field of molecular biology have provided a wide spectrum of methods suitable for target identification. The application of the Connectivity Map, developed by Golub and coworkers, which uses gene expression signature for profiling (Lamb et al., 2006), led to the identification of a class of HSP90 pathway modulators (gedunin and celastrol) (Hieronymus et al., 2006). Cell morphology-based profiling (Abassi et al., 2009; MacDonald et al., 2006) and activity-based proteomic profiling (Leung et al., 2003) are also used for molecular target identification.

Compared with gene expression profiling, which can simultaneously measure the expression of more than 20,000 genes, proteome analysis provides us only with the opportunity to trace at most 1,000 protein spots. However, any change of molecular weight and isoelectric point of proteins after posttranslational modification is often detectable as a mobility shift of protein spots in two-dimensional gel electrophoresis (2DE) analyses. Because biologically active compounds affect cellular processes and induce changes in both expression level and modification of proteins, proteome profiling is an informative approach for investigating the effects of a compound. Indeed, several research groups have shown that a biologically active compound alters the proteome (Cecconi et al., 2007; Towbin et al., 2003). Recent advances in two-dimensional difference gel electrophoresis (2D-DIGE) have allowed the measurement of the abundance of each protein spot between different gels with high accuracy due to introduction of an internal standard (Van den Bergh and Arckens, 2004). With 2D-DIGE, the abundant proteomic expression data obtained from different treatments can be collected and the expression patterns can be compared. In this study, we have used 2D-DIGE to perform a comprehensive proteome analysis of protein expression changes caused by the treatment of cancer cells with anticancer drugs claimed to possess the exact mechanisms of action.

It is well known that the anticancer drugs of known and similar mechanisms of action such as doxorubicin and daunorubicin, both classified as anthracyclines, are clinically active against different types of cancers. Doxorubicin is mainly used in the treatment of solid tumors, whereas daunorubicin shows activity in hematologic malignancies. Another case is cisplatin and oxaliplatin, the former active against lung and ovarian cancers and the latter active against colon cancer. Keeping in mind a subtle difference in clinical activity of the compounds of similar exact mechanism of action, we have made an attempt to establish differential protein profiles in cancer cells treated with anticancer agents representing several main mechanisms of action, including also several compounds possessing the same well-established mechanism of action. The proteomic profiling of mechanism of action may play an essential role in the planning of individualized chemotherapy of cancer patients once the correlation between drug sensitivity and the drug-induced proteomic profile is found.

Here we report the procedure and results of the proteome analysis using 2D-DIGE that revealed significant similarities in protein expression changes induced by the compounds belonging to the same class. Furthermore, we were also able to distinguish subtle differences among compounds attacking the same molecular target, though in a different way.

RESULTS

Proteomic Patterns of Geldanamycin- and Radicicol-Treated HeLa Cells Are Similar

Geldanamycin (**1**) and radicicol (**2**) are well-known HSP90 inhibitors (Schulte et al., 1998; Whitesell et al., 1994). HSP90 is a target for cancer therapeutics, and 17-AAG is a derivative of geldanamycin undergoing clinical trials (Nowakowski et al., 2006). First, we determined the cell growth inhibitory effect of HSP90 inhibitors against HeLa cells using a WST-8 assay (Figure 1A). The 50% growth inhibitory concentration (IC_{50}) of geldanamycin against HeLa cells was approximately 0.05 μM in a 48 hr treatment. HeLa cell growth was not affected at concentrations lower than 0.01 μM, whereas complete growth inhibition was observed at concentrations greater than 0.1 μM. The IC_{50} of radicicol against HeLa cell growth was approximately 1 μM.

Next, we investigated the relationship between proteomic changes after exposing HeLa cells to effective concentrations of the compounds, 0.005, 0.05, 0.5, 5, and 10 μM for geldanamycin and 10 μM for radicicol; the results are shown in Figure 1B. In this analysis, 775 spots in 2DE gels were matched on all gel images and quantified by 2D-DIGE system software, resulting in 282 spots that were selected by ANOVA (p < 0.01) and Dunnett's test (p < 0.01) (see Table S1 available online). Then, hierarchical cluster analysis was performed. The results are displayed in the form of a heat map and a tree diagram (Figure 1B). In the heat map, the spots with increased expression are indicated in red, and the spots with decreased expression are indicated in green. As indicated in the tree diagram and the heat map, the patterns of protein expression were similar at geldanamycin concentrations greater than 0.5 μM.

To simplify the statistical evaluation of the 2D-DIGE experiments, the spots that were modified significantly between groups were typically selected using the ANOVA test and a volume ratio filter of no less than 2-fold for three biological replicates per group (Karp and Lilley, 2005). Using these parameters, 17 spots were selected and a similar result for the cluster analysis was obtained (data not shown).

HSP70 and HSP27 have been reported to be upregulated in HSP90 inhibitor-treated cells (Maloney et al., 2007; McCollum et al., 2006). To classify test compounds using proteomic profiling, the identity of each protein spot is not necessary; however, it is important to confirm whether a proteomic change of geldanamycin-treated cells matches that in previously reported results. Peptide mass fingerprinting identified 20 spots out of the total number of spots that had been significantly affected by the treatment with geldanamycin and other compounds (Tables S2 and S3). The application of the ANOVA test selected 15 out of 20 spots and the mean ratios between control and inhibitor-treated cells were tabulated (Table 1).

Spots 1114 and 1127, which were identified as heat shock 70 kDa protein 1 (HSP70, *HSPA1B*), were upregulated more than 7-fold when compared with control. At 0.05 μM geldanamycin, HSP70 upregulation was also detected, but the magnitude of increase was lower compared with higher concentrations. The expression level of spot 2382, identified as heat shock protein β-1 (HSP27, *HSPB1*), also reached a plateau, as did HSP70. By western blot, both HSP70 and HSP27 were upregulated to similar extents at concentrations greater than 0.05 μM (Figure 1C).

The upregulation of mitochondrial heat shock proteins (*HSP9B*, *HSPD1*) and protein disulfide isomerase and downregulation of eukaryotic elongation factor 2 (*EEF2*), fascin (*FSCN1*), adenylyl cyclase-associated protein 1 (*CAP1*), and aldo-keto reductase family 1 member C2 (*AKR1C2*) were observed in geldanamycin-treated HeLa cells. It is very important to note that the concentration corresponding to the IC_{50} in the WST-8 assay is insufficient to induce any obvious changes in the proteomic analysis. It is more reasonable to use concentrations at which cell growth is nearly completely inhibited.

When the cells were exposed to 0.5 μM geldanamycin, the amount of HSP70 increased in a time-dependent manner and reached a plateau after 18 hr (Figures 1D and 1E). Because long incubation with test compounds may be associated with secondary effects such as apoptosis, we purposely avoided long exposures. Instead, we performed a subsequent proteomic analysis of HeLa cells after 18 hr exposure to a test compound.

Radicicol (**2**) is another HSP90 inhibitor that structurally differs from geldanamycin (**1**). The expression patterns between radicicol- and geldanamycin-treated cells were compared by 2D-DIGE. Similar responses were observed between geldanamycin- and radicicol-treated cells (Figure 1B; Table 2). HSP70 (1114 and 1127), HSP27 (2372 and 2382), and 78 kDa glucose-regulated protein (GRP78, *HSPA5*; 972 and 983) increased during both treatments (Table 2). The spots representing eukaryotic elongation factor 2, fascin, and adenylyl cyclase-associated protein 1 were downregulated during both treatments. These results strongly suggest that compounds inhibiting the same molecular target generate similar proteomic profiles.

Proteomic Analysis of HeLa Cells Treated with Compounds of Known Mechanisms of Action

To compare proteomic patterns in HeLa cells treated with compounds whose targets are known, well-characterized
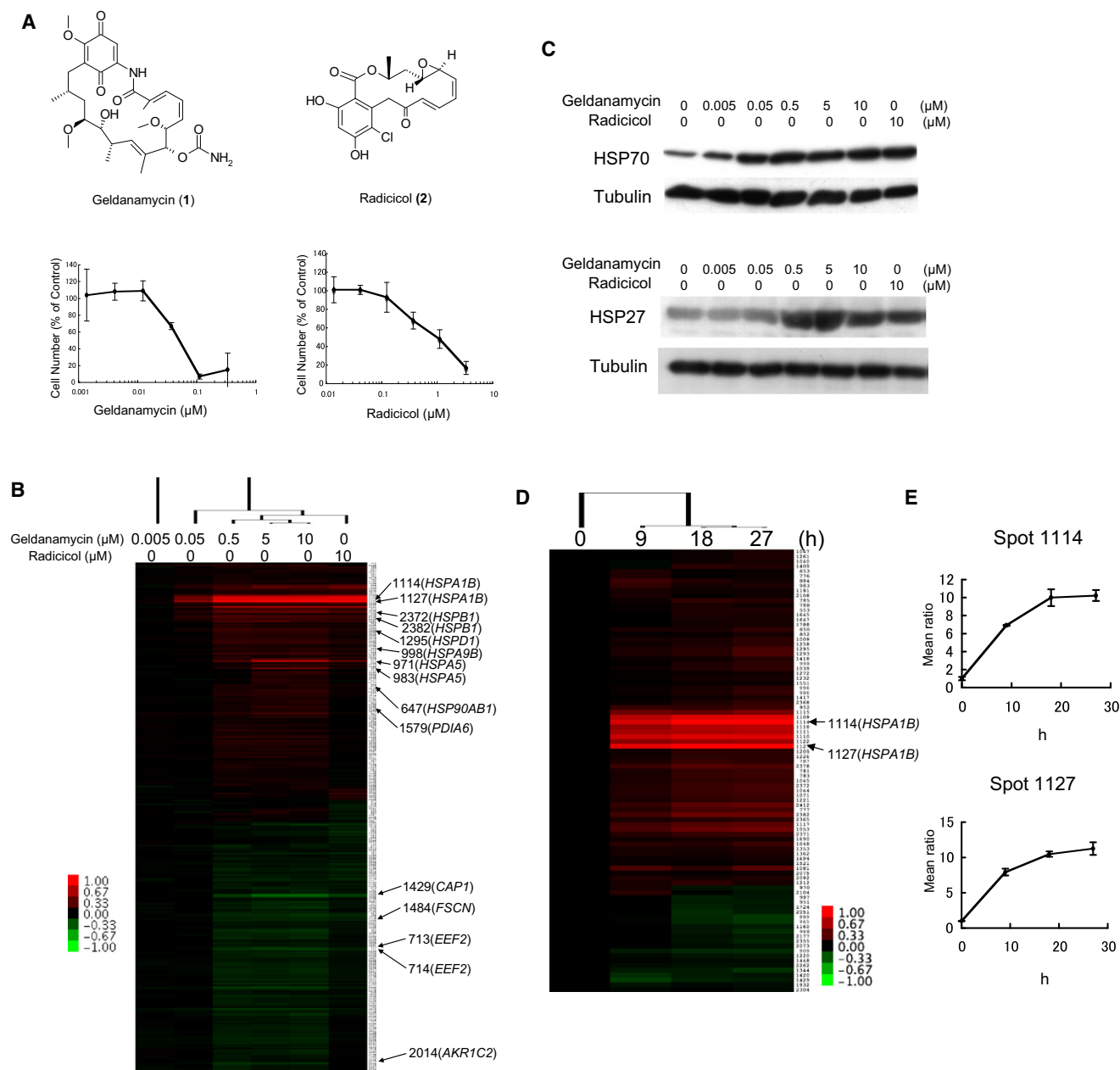
Figure 1. Dose- and Time-Dependent Effects of Geldanamycin and Radicicol on HeLa Cells

(A) Geldanamycin or radicicol was added at the indicated concentrations and incubated for 48 hr. Cell number was measured by WST-8 assay, as described in Experimental Procedures. Error bars represent SD (n = 3).

(B) HeLa cells treated with a compound at the indicated concentrations or with DMSO for 18 hr were analyzed by 2D-DIGE. Hierarchical clustering was performed. Red, upregulated; green, downregulated. The spots identified by peptide mass fingerprinting (PMF) (Table S2) are indicated by an arrow, and the master number and gene name are shown.

(C) Cell lysates incubated for 18 hr with designated concentrations of geldanamycin or radicicol were analyzed by western blot following SDS-PAGE using anti-HSP70, anti-HSP27, or anti-tubulin.

(D) HeLa cells were incubated in the presence of 0.5 μM geldanamycin for the indicated times and analyzed by 2D DIGE. Using the data of 91 spots selected as described in Experimental Procedures, hierarchical clustering was performed. The spots designated by the arrows are the spots (1114 and 1127) identified as HSP70 by PMF.

(E) Mean ratios of spots 1114 and 1127, determined in (D), were plotted. Error bars represent SD (n = 3).

chemical entities were selected for proteomic analysis (Table 2). Based on experience with geldanamycin, the proteomic analysis of above-mentioned compounds was performed at concentra-

tions higher than their respective IC$_{50}$ values. Their growth inhibitory effects were determined by WST-8 assay and are presented as IC$_{50}$ values in Table 2. The concentrations used for the

Table 1. Expression Data of Identified Spots in HeLa Cells Treated with Geldanamycin or Radicicol

Compounds	Master Number of Spots and Gene Name of Identified Proteins														
	673	713	714	971	983	998	1114	1127	1295	1429	1484	1579	2014	2372	2382
	HSP90AB1	EEF2	EEF2	HSPA5	HSPA5	HSPA9B	HSPA1B	HSPA1B	HSPD1	CAP1	FSCN1	PDIA6	AKR1C2	HSPB1	HSPB1
Geldanamycin 0.005 μM	1.02	0.97	0.95	1.03	1.01	0.95	1.05	1.10	1.02	0.96	0.97	1.04	0.95	1.04	0.98
Geldanamycin 0.05 μM	0.97	0.93	0.95	1.07	1.04	1.03	2.74**	3.40**	1.19*	0.96	0.96	1.02	0.91*	1.41*	1.43**
Geldanamycin 0.5 μM	1.29**	0.71**	0.63**	2.26**	1.29*	1.39**	7.22**	8.94**	1.75**	0.61**	0.71**	1.19**	0.66**	2.38**	1.90**
Geldanamycin 5 μM	1.31**	0.66**	0.59**	5.90**	2.70**	1.31**	7.33**	9.20**	1.62**	0.39**	0.72**	1.44**	0.69**	2.48**	1.82**
Geldanamycin 10 μM	1.41**	0.70**	0.55**	5.72**	2.71**	1.41**	8.05**	9.26**	1.64**	0.40**	0.71**	1.42**	0.66**	2.64**	1.75**
Radicicol 10 μM	1.19*	0.82*	0.72**	2.60**	1.28*	1.28*	7.43**	9.39**	1.34**	0.55**	0.75**	1.07	1.06	2.11**	1.65**

The mean ratios of identified spots between control and compound-treated cells are listed. Non-repeated-measures ANOVA and Dunnett's test for post hoc analysis were performed. Asterisks indicate significant differences from respective controls (*$p < 0.05$, **$p < 0.01$).

exposure of HeLa cells during proteomic profiling experiments were those inhibiting cell growth by 80% or more (Table 2).

As previously indicated, proteomic analyses of HeLa cells were performed after an 18 hr exposure to a test compound. Because the master gel of geldanamycin-treated cells from the previous experiment (Figure 2A) was used as the template, the numbering of the spots remained the same in all experiments. Three hundred eighteen spots in the 2DE gel were matched on all gel images and quantified by 2D-DIGE software; 298 of them were selected by ANOVA ($p < 0.01$) and Dunnett's test ($p < 0.01$) (see Table S4). The data were calculated and visualized by cluster analysis programs (Figure 2B); the mean ratio of the identified spots and the results of statistical analysis are listed in Table S4.

As indicated in the tree diagram (Figure 2B), the inhibitors of V-ATPase (bafilomycin A1 and concanamycin A), tubulin (nocodazole and vinblastine), and actin (cytochalasin D and jasplakinolide) were classified into separate clusters. The spots that changed significantly between groups were selected using ANOVA and a volume ratio filter of no less than 2-fold (Karp and Lilley, 2005), yielding 47 spots and leading to a similar result of cluster analysis (data not shown).

We also noticed that MG-132, a proteasome inhibitor, generated a similar pattern as the HSP90 inhibitors did. The amount of

Table 2. Compounds for Proteomic Analysis by 2D-DIGE

Compounds	Target	IC$_{50}$ (μM)[a]	Concentration (μM)[b]	References
Actinomycin D	RNA synthesis	0.0022	0.015	Sobell, 1985
Bafilomycin A1	V-ATPase	0.0035	0.01	Bowman et al., 1988
Brefeldin A	Protein transport	0.023	0.05	Klausner et al., 1992
Concanamycin A	V-ATPase	0.002	0.005	Huss et al., 2002
Cycloheximide	Protein synthesis	0.17	2	Obrig et al., 1971
Cytochalasin D	Actin	0.32	1	Cooper, 1987
Daunomycin	DNA synthesis	0.034	1	Aubel-Sadron and Londos-Gagliardi, 1984
Etoposide	Topoisomerase II	3	50	Liu, 1989
Geldanamycin	HSP90	0.18	0.5	Whitesell et al., 1994
ICRF-193	Topoisomerase II	2	50	Roca et al., 1994
Jasplakinolide	Actin	0.038	0.1	Bubb et al., 1994
LY294002	PI3 kinase	12	42	Vlahos et al., 1994
MG-132	Proteasome	0.24	1	Lee and Goldberg, 1998
Nocodazole	Tubulin	0.027	5	Lin and Hamel, 1981
Okadaic acid	Phosphatase	0.014	0.03	Bialojan and Takai, 1988
Radicicol	HSP90	2.1	10	Schulte et al., 1998
Staurosporine	Protein kinase	0.03	0.3	Rüegg and Burgess, 1989
Tunicamycin	N-linked oligosaccharide synthesis	0.27	5	Takatsuki et al., 1971
Vinblastine	Tubulin	0.0031	0.01	Rai and Wolff, 1998

[a] The 50% inhibitory concentration of HeLa cell growth.
[b] Concentrations used for proteome analysis.

A

C

Iejimalide A (**3**)

Iejimalide B (**4**)

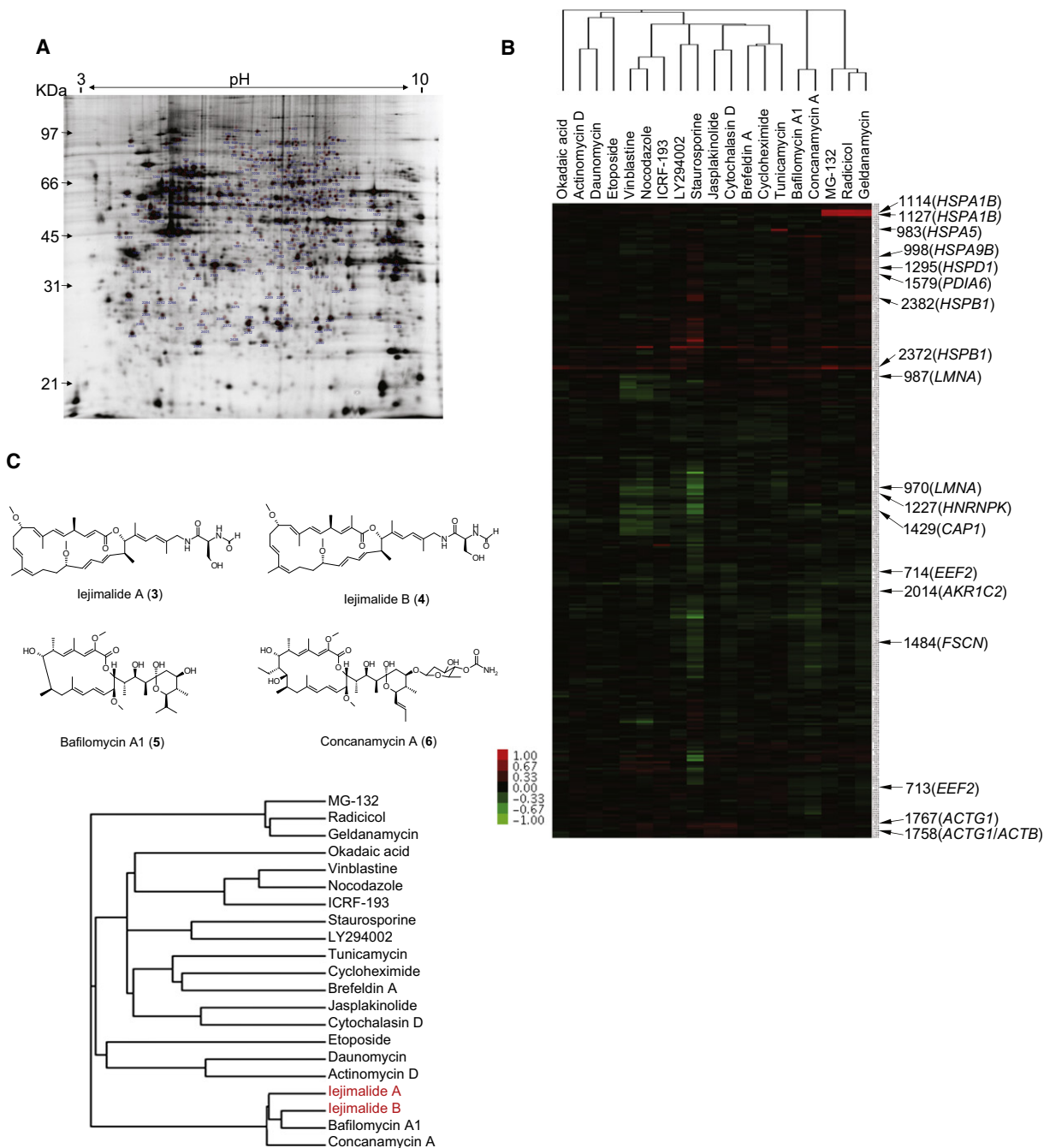Bafilomycin A1 (**5**)

Concanamycin A (**6**)

B

Figure 2. Clustering of Well-Characterized Compounds and Iejimalides by Proteomic Analysis of HeLa Cells

(A) HeLa cells treated with compounds listed in Table 2 for 18 hr were analyzed by 2D DIGE. The position of each spot is designated by a red circle, and the master number of the spot is marked.

(B) Hierarchical clustering was performed. The identified spots (Table 3) are designated by arrows.

(C) HeLa cells were treated with 30 nM iejimalides A and B. The quantitative data were combined with the data of 19 well-characterized compounds and hierarchical clustering was performed.

protein in the HSP70 spots (spots 1114 and 1127) also increased in MG-132-treated cells, as did those observed in geldanamycin- and radicicol-treated cells (Table 3). In contrast, HSP27 showed an aberrant pattern. Although HSP90 inhibitors increased in amount in spots 2372 and 2382, which were identi-

fied as HSP27, MG-132 treatment increased only in spot number 2372.

Other noteworthy changes were as follows: (1) the inhibitors of actin, cytochalasin D, and jasplakinolide increased the amount of actin (spots 1758 and 1767); (2) tunicamycin increased in

Table 3. Expression Data of Identified Spots on HeLa Cells Treated with Well-Characterized Compounds

Compounds	Master Number of Spots and Gene Name of Identified Proteins																	
	713	714	970	983	987	998	1114	1127	1227	1295	1429	1484	1579	1758	1767	2014	2372	2382
	EEF2	EEF2	LMNA	HSPA5	LMNA	HSPA9B	HSPA1B	HSPA1B	HNRNPK	HSPD1	CAP1	FSCN1	PDIA6	ACTG1/ACTB	ACTG1	AKRLC2	HSPB1	HSPB1
Okadaic acid	0.97	0.79*	0.86	1.10	0.97	1.12	1.30	1.22	0.88	1.12	0.61**	1.05	1.03	0.92	1.05	1.12*	2.31**	0.77**
Actinomycin D	1.12	1.12	1.16	1.01	1.29**	0.96	1.02	1.12	0.91	0.99	0.74**	1.12	1.06	0.99	1.04	1.11	1.83**	1.08
Daunomycin	1.18	1.08	1.18	0.97	1.59**	0.92	1.02	1.06	0.90	0.93	0.97	0.92	1.09	0.82	0.91	0.96	1.63**	1.03
Etoposide	1.05	1.05	1.09	1.04	1.19	1.05	1.14	1.16	1.02	1.03	1.06	0.92	1.06	0.99	0.95	0.86*	1.81**	0.93
Vinblastine	0.96	1.01	0.49**	0.83*	0.49**	1.09	1.51	1.10	0.47**	0.97	0.49**	1.04	0.95	1.19	1.32**	1.05	1.61**	0.91
Nocodazole	0.95	0.87	0.41**	0.86	0.59**	1.12	1.40	1.04	0.48**	0.92	0.43**	1.00	0.96	1.20	1.61**	0.81**	2.11**	0.89
ICRF-193	0.93	0.90	0.60**	0.87	0.59**	1.14	1.38	1.28	0.69**	1.01	0.62**	0.93	1.02	1.04	1.17	0.94	1.58**	1.04
LY294002	1.06	0.87	0.88	1.08	1.14	1.08	1.00	0.87	0.63**	0.93	0.62**	0.71**	1.12	0.96	1.11	0.89	2.08**	0.99
Staurosporine	0.90	0.67**	0.28**	1.71**	0.87	1.40**	1.07	0.80	0.31**	1.42**	0.33**	0.58**	1.07	0.97	1.42**	1.09	1.03	2.30**
Jasplakinolide	1.08	0.94	0.84	0.88	0.94	0.98	1.09	0.89	0.90	0.80**	1.22**	1.06	0.97	1.54**	1.93**	0.83**	1.04	1.07
Cytochalasin D	1.07	0.80*	0.90	0.83*	1.04	1.05	1.10	0.74	0.86	0.79**	1.10*	0.77**	0.94	1.25*	1.86**	0.75**	1.20	0.80**
Brefeldin A	1.07	0.98	0.91	1.25**	0.99	1.01	0.94	0.93	0.89	0.78**	0.97	0.87*	0.96	0.94	0.96	0.95	1.55**	0.88
Cycloheximide	1.21*	1.09	0.87	0.70**	1.05	0.90	0.90	0.78	0.82**	0.79**	0.95	0.92	0.90	0.96	1.15	0.90	1.88**	0.85
Tunicamycin	1.19*	1.10	0.72**	4.62**	0.85	1.02	0.94	0.80	0.75**	0.82**	0.81**	0.93	1.11	1.13	1.22	1.04	1.67**	0.86*
Bafilomycin A1	0.79*	0.71**	1.38**	1.31**	1.71**	1.25**	0.93	0.85	1.23**	1.23**	0.62**	0.61**	1.19**	0.84	1.01	0.68**	2.25**	0.99
Concanamycin A	0.85	0.74**	1.23*	1.02	1.50**	1.04	0.91	0.81	1.07	0.99	0.72**	0.76**	0.99	0.84	0.99	0.67**	2.03**	0.85**
MG-132	0.92	0.82*	0.91	1.40**	1.10	1.10	7.18**	6.84**	0.78**	1.10	0.90*	0.69**	1.04	0.93	0.98	0.84**	4.01**	0.93
Radicicol	0.82	0.72**	0.75**	1.28**	0.70**	1.28**	7.43**	9.39**	0.88	1.34**	0.55**	0.75**	1.07	0.95	1.18	1.06	2.11**	1.65**
Geldanamycin	0.71**	0.63**	1.02	1.29**	0.95	1.39**	7.22**	8.94**	1.09	1.75**	0.61**	0.71**	1.19**	1.04	1.08	0.66**	2.38**	1.90**

The mean ratios of identified spots between control and compound-treated cells are listed. Non-repeated-measures ANOVA and Dunnett's test for post hoc analysis were performed. Asterisks indicate significant differences from respective controls (*p < 0.05, ** p < 0.01). The order of compounds follows that in Figure 2B.
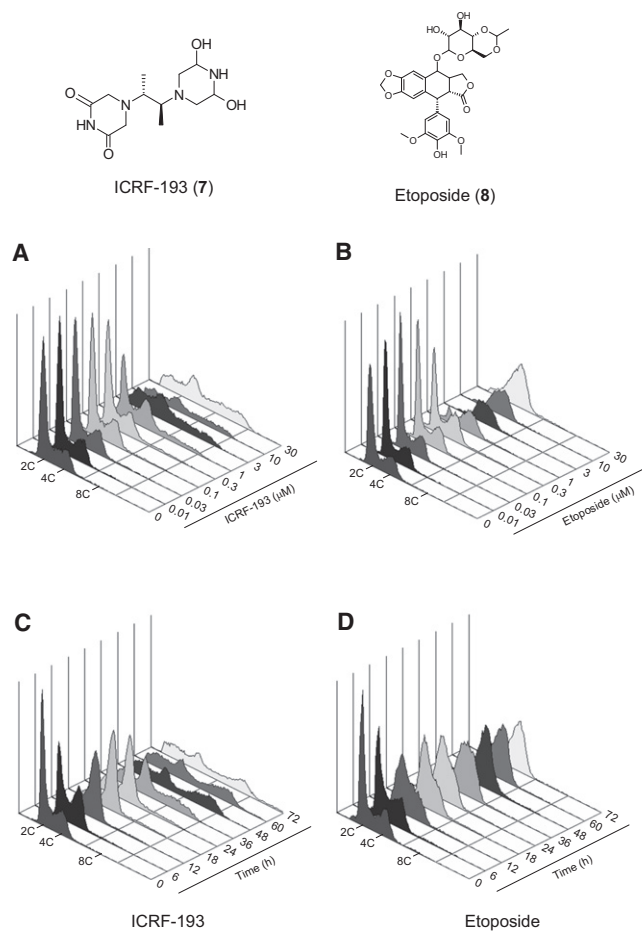
ICRF-193 (**7**)

Etoposide (**8**)

Figure 3. Differential Phenotypes of HeLa Cells Treated with ICRF-193 and Etoposide by Flow Cytometry
The distribution of cellular DNA content of asynchronous HeLa cells treated with ICRF-193 or etoposide was determined by flow cytometry. HeLa cells were treated with the indicated concentrations of ICRF-193 (A) or etoposide (B) for 48 hr. In a time course experiment, HeLa cells were treated with 10 μM ICRF-193 (C) or etoposide (D) for the indicated times.

spot 983, identified as GRP78, 4.6-fold compared with control; (3) ICRF-193 and antimicrotubular agents such as nocodazole and vinblastine decreased the amount of lamin (spots 970 and 978), in consequence forming one cluster; and (4) the potent protein kinase inhibitor staurosporine downsized the spots 714 (*EEF2*), 970 (*LMNA*), 1227 (*HNRNPK*), 1429 (*CAP1*), and 1484 (*FSCN1*), whereas expanding the spots 983 (*HSPA5*), 998 (*HSPA9B*), 1295 (*HSPD1*), 1767 (*ACTG1*), and 2382 (*HSPB1*).

Iejimalides, 24-membered macrolides, were originally isolated from marine tunicate as potent antitumor compounds (Nozawa et al., 2006). We recently found that iejimalides inhibited V-ATPase (Kazami et al., 2006). We have analyzed HeLa cells treated with iejimalide A (**3**) or iejimalide B (**4**) at 30 nM by 2D-DIGE. We combined the proteome data from iejimalide-treated HeLa and compared them with the proteomic profiles generated by the treatment of HeLa cells with 19 well-characterized compounds. Iejimalide A (**3**) and B (**4**) were clustered into the same tree as the other V-ATPase inhibitors (e.g., bafilomycin A1

[**5**] and concanamycin A [**6**]) (Figure 2C). Recently, it was reported that iejimalides affect actin depolymerization (Fürstner et al., 2007); however, iejimalides A and B did not match the cluster representing actin inhibitors. These results indicate that the primary target of iejimalides in HeLa cells is V-ATPase, at least at the concentration used in our experimental setting.

Flow Cytometry of HeLa Cells Treated with ICRF-193 and Etoposide

The proteomic analysis of HeLa cells treated with the two structurally different inhibitors of topoisomerase II (topo II), ICRF-193 (**7**) and etoposide (**8**), revealed significant differences; the two compounds were not able to form a single cluster (Figure 2B). To confirm this finding, we measured the distribution of cellular DNA in HeLa cells by flow cytometry after treating asynchronous HeLa cells with varying concentrations of ICRF-193 or etoposide for 48 hr.

The basic amount of DNA in a haploid nucleus is given the value C. In the absence of inhibitors, we typically observed two peaks, corresponding to cell populations with 2C and 4C DNA content. The treatment of HeLa cells with ICRF-193 resulted in decreasing the height of the 2C peaks at concentrations higher than 1 μM, while the 4C population increased (Figure 3A). On the other hand, etoposide used at concentrations higher than 1 μM also increased the 4C peaks, but without any obvious accumulation of the peaks containing 8C DNA, in contrast to the effect of ICRF-193 (Figure 3B).

The kinetics of the shifts from the diploid to tetraploid DNA cellular contents was also studied in a time-dependent fashion, using equimolar concentrations of 10 μM for both test compounds. ICRF-193 induced a gradual accumulation of 4C population up to 18 hr, and then the generation of polyploidy (8C) in HeLa cells was observed (Figure 3C) beyond that time point.

Etoposide was not able to induce polyploidy in HeLa cells, even during a 72 h exposure (Figure 3D). Despite the presence of a common mechanism of action (topo II inhibition), the final biological effects were different, and the two compounds were clustered into a different cluster in our proteomic analysis.

DISCUSSION

In this study, we have performed a proteomic analysis of HeLa cancer cells treated with well-characterized anticancer agents using a 2D-DIGE system. The target proteins of these compounds are known at the cellular level and represent targets for cancer therapeutics such as the proteasome and microtubules. Each compound induced a characteristic proteomic pattern, and hierarchical clustering exactly classified the compounds according to their respective targets, such as HSP90, tubulin, and V-ATPase (Figure 2B).

Topo II inhibitors are still good candidates for molecular targeted drugs in cancer therapy. Topo II as a single target can be inhibited by two distinct mechanisms. One is exercised by a catalytic site inhibition, resulting in the formation of a noncleavable complex and is characteristic for ICRF-193, a topo II inhibitor (**7**) (Roca et al., 1994; Tanabe et al., 1991). The other mechanism involves the stabilization of a DNA-cleavable complex, which further leads to double-strand DNA breaks

and damage; etoposide (**8**), a topo II poison, plays an essential role in this mechanism (Liu, 1989). As reported by Ishida et al., etoposide blocked the progression of cells to M phase, whereas ICRF-193 only delayed the transition from S to M phase and induced polyploidization in HeLa cells (Ishida et al., 1994). Thus, both compounds are topo II inhibitors but act through disparate mechanisms (Andoh and Ishida, 1998). Their proteomic phenotypes differed and did not fall into the same cluster. Moreover, their cellular phenotypes, as determined by the analysis of cellular DNA distribution (Figure 3), differed as well. One may conclude that such compounds can be classified into different clusters from a proteomic point of view, despite exercising their biological activity through the same molecular target, or their exact mechanism of action may be revised. An inability to share a common cluster might be caused by an excessive off-target effect. To clarify this matter, it seems important to know which mechanism determines anticancer activity against a particular type of cancer or contributes mainly to toxicity. Gathering more data will be of great importance in the evaluation of undesired effects as well.

So far, our proteomic profiling of mechanisms of action of anticancer agents appeared to be helpful in the identification of the mode of action of iejimalides, newly isolated natural products, as being inhibitors of V-ATPase (Figure 2C). The comparison of the proteomes of cells treated with a newly isolated compound versus well-characterized compounds can lead to a testable hypothesis on general mechanisms of action as in the case of other profiling approaches such as the genetic one.

Despite recent enthusiasm, one may anticipate certain limitations of our proteome profiling system. To name a few, the following factors may become obstacles in the system. (1) The suspected target for a test compound is not expressed or is not functional (mutation, single-nucleotide polymorphism) in HeLa cells. (2) The suspected target was not validated yet by known standards. (3) The changes induced in the proteomic profile by a test compound are not sufficiently distinct due to the appearance of a limited number of spots in 2D gels. (4) The presence of several molecular targets may complicate the analysis; therefore, an interpretation of the data will have to be made with great caution.

Our proteomic analysis matched methyl-gerfelin with two V-ATPase inhibitors; however, its biological effects in a cell system (upregulation of pH) (Figure S1) were not confirmed. Our newly developed technology of a small-molecule affinity matrix revealed a strong interaction with glyoxalase I, supposedly a direct target molecule (Kawatani et al., 2008). The lack of standards for glyoxalase I inhibitors in proteomic analysis led to clustering with V-ATPase inhibitors. Therefore, the expansion of the system by a variety of compounds with increased precision and accuracy in classifying compounds into groups will lead to a well-established mechanism of action. Compounds not matching any known mechanisms may be considered as probes for searching molecular targets not yet identified.

The case of jasplakinolide and cytochalasin D may well illustrate some of the obstacles, as both compounds affect actin by inhibiting its depolymerization (Bubb et al., 1994) and polymerization (Cooper, 1987), respectively. Although their effects on actin are opposed, both compounds increased the levels of actin and were included in the same cluster in this experiment.

However, we noted the presence of several unidentified spots that did not correlate to these two compounds. Further investigation should clarify differences between polymerizing and depolymerizing effects of these two inhibitors with the application of proteomic analysis.

2DE-based proteomic analysis is generally a time-consuming process during the initial stage of system development, because the identification of almost all protein spots is essential. Once this stage is completed and a database is created, one can analyze the proteomic profiles of many chemical entities by comparing them with those contained in the database, without the necessity of additional protein spot identification. This is a huge advantage of this technique. Nevertheless, in the case of dramatic changes in expression levels among spots not yet identified, the characterization of these spots will be very informative in target identification, or at least these compound-specific spots may serve as an important marker of biological activity. Agents inducing microtubule depolymerization may serve as an illustration of where a compound does not directly cause the modification of a protein spot, and is rather an artifact related to its primary mechanism of action. More specifically, antimicrotubular agents cause cell-cycle arrest in M phase, preventing cell division due to the lack mitotic spindle formation, and the nuclear envelope remains intact. Under normal conditions the envelope is broken down and its component, lamin, is released (Parnaik, 2008). The release of lamin is decreased after the exposure of the cells to antimicrotubular agents (Table 3) and may serve as a marker of compound's effectiveness, albeit not being a target.

The treatment of HeLa cells with MG-132 increased the expression of HSP70, thus confirming already reported phenomena (Kawazoe et al., 1998), and the cluster analysis tree positioned this compound close to the group of HSP90 inhibitors. However, slight differences were observed, namely, HSP90 inhibitors increased both spots of HSP27 (2372 and 2382), whereas MG-132 increased only spot 2372. Because HSP27 has been reported to enhance proteasome-dependent protein degradation (Parcellier et al., 2003, 2006), this result may suggest the presence of at least two forms of HSP27, one of which is probably involved in proteasome-dependent protein degradation. Based on these results, we propose that the expression levels of HSP27 spots may determine the classification of compounds either to the HSP90 inhibitor or to the proteasome inhibitor class of compounds. Particularly, the expression ratio of HSP70 and HSP27 spots will play the role of differentiating marker for either class.

So far, we have examined only 19 compounds, reaching an ability to classify the compounds according to their mechanism of action. The expansion of proteomic profiling by the other types of compounds with different modes of action will make the system fully operational for the prediction of biological activity of newly discovered natural products or synthetic compounds. Already, we have been able to classify a newly synthesized derivative of a natural product with an unknown mechanism of action as an inhibitor of topoisomerase II (data not shown). For that purpose, the extensive process of system validation using the chemical library of NPDepo (Tomiki et al., 2006) is under way. Because the assay is primarily based upon only one cancer cell line, it is reasonable to include other cell lines, especially

when obvious differences in drug responses among cell lines are observed. As the natural consequence of the recent promising results, there is the need to include a protein interaction map that should enforce the discovery of new target molecules. One may easily indicate a protein spot which may become a marker; however, one should explore the path from the marker up to the protein responsible for that change. Then the protein may be claimed to be a target or, in other words, the object of a primary attack by an active substance.

In summary, proteomic profiling based on 2D-DIGE is an important supplement to other multidimensional phenotypic profilings and its capacity may be extended by the introduction of different pathological phenotypes represented by cancer cells, leading, for example, to identification of specific biomolecules as well.

SIGNIFICANCE

New natural compounds, possessing important biological activity, have been subjected to extensive and time-consuming processes to clarify main mechanisms of action. In order to reduce the time for target identification, we set up a faster method based on 2D-PAGE characteristic proteomic patterns of HeLa cells treated with various compounds. Compounds such as geldanamycin and radicicol, representing diverse structures but sharing a common target, were classified in the same tree by cluster analysis. Iejimalides A and B were reported to affect depolymerization of actin; however, these were not clustered together with actin inhibitors but instead were clustered into a group of V-ATPase inhibitors, as has been confirmed by the direct inhibitory effect of iejimalides A and B on V-ATPase (Kazami et al., 2006). Furthermore, when different types of topo II inhibitors, etoposide and ICRF-193, which are known as a topo II poison and a catalytic inhibitor, respectively, were analyzed by the system, the compounds were clustered into different trees. This indicates a power of the system that discriminates compounds by mechanism of action. The expansion of the database of proteomic profiling by a 2D-PAGE assay will aid the characterization of numerous natural compounds in many aspects, such as mechanism of action, off-target effects, biomarking, and yet unknown target identification.

EXPERIMENTAL PROCEDURES

Materials

Iejimalides A and B were obtained from Dr. Jun'ichi Kobayashi of Hokkaido University. Actinomycin D, brefeldin A, concanamycin A, cycloheximide, cytochalasin D, geldanamycin, radicicol, staurosporine, and etoposide were provided by the NPDepo (RIKEN Natural Products Depository; http://www.npd.riken.jp/npd). Bafilomycin A1, daunomycin, and tunicamycin were purchased from Wako Pure Chemical Industries. Okadaic acid and nocodazole were purchased from Sigma. Jasplakinolide, LY294002, MG-132, and vinblastine were from Calbiochem. ICRF-193 was from Funakoshi.

All compounds were dissolved in dimethyl sulfoxide (DMSO) and stocked at −20°C. Monoclonal anti-HSP70 (clone C92F3A-5) and monoclonal anti-HSP27 (clone G3.1) were purchased from Stressgen Biotechnologies. Monoclonal anti-α-tubulin (clone DM1A) was purchased from Sigma. The reagents for western blotting were purchased from Thermo Scientific. All reagents were reagent grade.

Cell Culture

HeLa cells were cultured in Dulbecco's modified Eagle's medium, supplemented with 10% fetal bovine serum, at 37°C in a humidified CO_2 incubator (5% CO_2/95% air).

Cell Growth Assay

HeLa cells were seeded at 2×10^3 cells per well in a 96-well culture plate and incubated overnight; test compounds were added to the medium at various concentrations. After 48 hr, cell number was determined using Cell Count Reagent SF (Nakalai Tesuque) according to the manufacturer's protocol. Briefly, 10 μl of WST-8 solution (mixture of WST-8 and 1-methoxy-5-methyl-phenazinium methylsulfate) was added to the wells and incubated for 2 hr, and cell number was assessed by measuring the absorbance at 450 nm on a microplate reader (Bio-Rad).

Preparation of Cell Lysates for Proteomic Analysis

HeLa cells (3×10^5 cells) were seeded on a culture dish (35 mm diameter) containing 3 ml of medium and incubated overnight. Each assay was done in triplicate. The cells were exposed for 18 hr to the designated concentrations of test compounds. Cells were washed three times with ice-cold phosphate-buffered saline (PBS), removed by a rubber policeman, and collected by centrifugation at 4000 rpm for 3 min at 4°C in a microcentrifuge (Kubota 3700).

After being washed once with PBS, cells were suspended in sample buffer (7 M urea, 2 M thiourea, 4% CHAPS, 30 mM Tris, buffered to pH 8.5) for 2D-DIGE and disrupted with a TOMY UR-20P sonicator. Cell lysates were treated with 1.25 U/μl benzonase (Merck) for 60 min on ice and centrifuged at 12,000 rpm for 3 min at 4°C. Supernatants were stocked at −80°C until use.

Labeling of Cell Lysates and 2DE

Protein concentration was determined by the Bradford procedure using a protein assay kit from Bio-Rad. Fifty micrograms of protein was labeled with 200 pmol of CyDye DIGE Fluor minimal dyes (GE Healthcare) according to the manufacturer's instructions (Cy3 and Cy5 for samples and Cy2 for internal control, consisting of equal parts of all samples in an experiment).

Samples were applied by rehydration onto immobilized pH gradient (IPG) strips (24 cm, pH 3–10, nonlinear gradient; GE Healthcare) and subjected to isoelectrofocusing in an IPGphor IEF system (GE Healthcare). Strips were incubated in equilibration buffer (6 M urea, 30% glycerol, 2% SDS, 50 mM Tris-HCl [pH 8.8]) containing 1% DTT for 15 min and then incubated in the same buffer containing 2.5% iodoacetamide for 15 min. Strips were transferred to the tops of 10% polyacrylamide gels and electrophoresed overnight in a DALT Twelve apparatus (GE Healthcare).

After electrophoresis, gels were scanned using a Typhoon 9400 imager at 100 dpi resolution (GE Healthcare). Gel analysis was performed using DeCyder BVA 6.5 (GE Healthcare), a 2DE analysis software package, following the manufacturer's recommendations. The estimated number of spots for each codetection was set to 3000.

Experimental Design and Data Processing for 2DE Profiling

To perform visual 2DE protein profiling of compound-treated HeLa cells, experiments were divided into subsets. We used the spot number of the master gel as the common master number for all of the experiments. The gel that contained the most spots in the first experiment (analysis of HeLa cells treated with various concentrations of geldanamycin) was chosen as the master gel.

In a representative subset of experiments, we used three compounds and DMSO. HeLa cells were treated with these solutions, and proteomic analysis was performed. All samples of compound- and DMSO-treated cells were prepared in triplicate. Equal parts of all samples in a subset of experiments were labeled with Cy2 CyDye Fluor as an internal standard.

To match the common master numbers between subsets of experiments, image files were imported into the project file, including the master gel, and spot maps of the images were matched to the master gel image using the BVA modules of DeCyder 6.5. More than 650 spots were usually matched in all the analyzed gels of a subset. The volume of each spot was obtained as a ratio of the Cy3- or Cy5-labeled sample compared with the corresponding Cy2 signal of the internal standard. Then, the volume of each spot was

normalized using the average of the corresponding control values from the DMSO-treated HeLa cells.

Normalized volume data in subsets of experiments were combined, and only spots that did not lack data in any of the gels were selected. Subsequently, the spots that showed significant changes after compound treatment were selected by ANOVA (p < 0.01) and Dunnett's test for post hoc analysis. For cluster analysis, the normalized volumes were calculated using the means of uncentered correlation with centroid linkage using Cluster 3.0 (de Hoon et al., 2004) and visualized using Java Treeview (Saldanha, 2004).

Statistical calculations, such as nonrepeated-measures ANOVA and Dunnett's test for post hoc analysis (Sheskin, 2000), were performed using Microsoft Excel with a statistical macro (ystat2006; Igaku Tosho Shuppan) and R version 2.9.2 (http://cran.r-project.org).

Western Blotting

Cell lysates were resolved by 10% SDS-PAGE and transferred to PVDF membranes. Membranes were blocked with 5% nonfat dried milk in TBS-T buffer (10 mM Tris-HCl [pH 8.0], 150 mM NaCl, 0.05% Tween 20), followed by incubation with primary antibody (1:1000 dilution) in TBS-T. The detection was performed using horseradish peroxidase-labeled secondary antibodies (1:1000 dilution) and enhanced chemiluminescence detection reagent. The expression of tubulin was also measured and used as an internal control.

Flow Cytometry

Cells were treated with 0.25% trypsin for 5 min to remove them from the dish, washed with PBS, fixed in cold PBS containing 70% (v/v) ethanol, and stored at $-20°C$ overnight. Then, the cells were washed with PBS and incubated with a DNA-staining solution containing 50 μg/ml propidium iodide (Sigma) and 2 μg/ml RNase A at $4°C$ for 30 min. Total fluorescence intensities were determined by quantitative flow cytometry with Cytomics FC500 (Beckman Coulter).

SUPPLEMENTAL INFORMATION

Supplemental Information includes one figure and four tables and can be found with this article online at doi:10.1016/j.chembiol.2010.03.016.

REFERENCES

Abassi, Y.A., Xi, B., Zhang, W., Ye, P., Kirstein, S.L., Gaylord, M.R., Feinstein, S.C., Wang, X., and Xu, X. (2009). Kinetic cell-based morphological screening: prediction of mechanism of compound action and off-target effects. Chem. Biol. 16, 712–723.

Andoh, T., and Ishida, R. (1998). Catalytic inhibitors of DNA topoisomerase II. Biochim. Biophys. Acta 1400, 155–171.

Aubel-Sadron, G., and Londos-Gagliardi, D. (1984). Daunorubicin and doxorubicin, anthracycline antibiotics, a physicochemical and biological review. Biochimie 66, 333–352.

Baker, D.D., Chu, M., Oza, U., and Rajgarhia, V. (2007). The value of natural products to future pharmaceutical discovery. Nat. Prod. Rep. 24, 1225–1244.

Bialojan, C., and Takai, A. (1988). Inhibitory effect of a marine-sponge toxin, okadaic acid, on protein phosphatases. Specificity and kinetics. Biochem. J. 256, 283–290.

Bowman, E.J., Sievers, A., and Altendorf, K. (1988). Bafilomycins: a class of inhibitors of membrane ATPase from microorganisms, animal cells and plant cells. Proc. Natl. Acad. Sci. USA 85, 7972–7976.

Boyd, M.R., Farina, C., Belfiore, P., Gagliardi, S., Kim, J.W., Hayakawa, Y., Beutler, J.A., McKee, T.C., Bowman, B.J., and Bowman, E.J. (2001). Discovery of a novel antitumor benzolactone enamide class that selectively inhibits mammalian vacuolar-type (H$^+$)-ATPases. J. Pharmacol. Exp. Ther. 297, 114–120.

Bubb, M.R., Senderowicz, A.M., Sausville, E.A., Duncan, K.L., and Korn, E.D. (1994). Jasplakinolide, a cytotoxic natural product, induces actin polymerization and competitively inhibits the binding of phalloidin to F-actin. J. Biol. Chem. 269, 14869–14871.

Cecconi, D., Donadelli, M., Rinalducci, S., Zolla, L., Scupoli, M.T., Scarpa, A., Palmieri, M., and Righetti, P.G. (2007). Proteomic analysis of pancreatic endocrine tumor cell lines treated with the histone deacetylase inhibitor trichostatin A. Proteomics 7, 1644–1653.

Cooper, J.A. (1987). Effects of cytochalasin and phalloidin on actin. J. Cell Biol. 105, 1473–1478.

de Hoon, M.J., Imoto, S., Nolan, J., and Miyano, S. (2004). Open source clustering software. Bioinformatics 20, 1453–1454.

Fürstner, A., Nevado, C., Waser, M., Tremblay, M., Chevrier, C., Teply, F., Aissa, C., Moulin, E., and Muller, O. (2007). Total synthesis of iejimalide A–D and assessment of the remarkable actin-depolymerizing capacity of these polyene macrolides. J. Am. Chem. Soc. 129, 9150–9161.

Hieronymus, H., Lamb, J., Ross, K.N., Peng, X.P., Clement, C., Rodina, A., Nieto, M., Du, J., Stegmaier, K., Raj, S.M., et al. (2006). Gene expression signature-based chemical genomic prediction identifies a novel class of HSP90 pathway modulators. Cancer Cell 10, 321–330.

Huss, M., Ingenhorst, G., König, S., Gassel, M., Dröse, S., Zeeck, A., Altendorf, K., and Wieczorek, H. (2002). Concanamycin A, the specific inhibitor of V-ATPases, binds to the V(o) subunit c. J. Biol. Chem. 277, 40544–40548.

Ishida, R., Sato, M., Narita, T., Utsumi, K.R., Nishimoto, T., Morita, T., Nagata, H., and Andoh, T. (1994). Inhibition of DNA topoisomerase II by ICRF-193 induces polyploidization by uncoupling chromosome dynamics from other cell cycle events. J. Cell Biol. 126, 1341–1351.

Kakeya, H., Onose, R., Koshino, H., Yoshida, A., Kobayashi, K., Kageyama, S., and Osada, H. (2002). Epoxyquinol A, a highly functionalized pentaketide dimer with antiangiogenic activity isolated from fungal metabolites. J. Am. Chem. Soc. 124, 3496–3497.

Karp, N.A., and Lilley, K.S. (2005). Maximising sensitivity for detecting changes in protein expression: experimental design using minimal CyDyes. Proteomics 5, 3105–3115.

Kawada, M., Momose, I., Someno, T., Tsujiuchi, G., and Ikeda, D. (2009). New atpenins, NBRI23477 A and B, inhibit the growth of human prostate cancer cells. J. Antibiot. (Tokyo) 62, 243–246.

Kawatani, M., Okumura, H., Honda, K., Kanoh, N., Muroi, M., Dohmae, N., Takami, M., Kitagawa, M., Futamura, Y., Imoto, M., and Osada, H. (2008). The identification of an osteoclastogenesis inhibitor through the inhibition of glyoxalase I. Proc. Natl. Acad. Sci. USA 105, 11691–11696.

Kawazoe, Y., Nakai, A., Tanabe, M., and Nagata, K. (1998). Proteasome inhibition leads to the activation of all members of the heat-shock-factor family. Eur. J. Biochem. 255, 356–362.

Kazami, S., Muroi, M., Kawatani, M., Kubota, T., Usui, T., Kobayashi, J., and Osada, H. (2006). Iejimalides show anti-osteoclast activity via V-ATPase inhibition. Biosci. Biotechnol. Biochem. 70, 1364–1370.

Klausner, R.D., Donaldson, J.G., and Lippincott-Schwartz, J. (1992). Brefeldin A: insights into the control of membrane traffic and organelle structure. J. Cell Biol. 116, 1071–1080.

Lamb, J., Crawford, E.D., Peck, D., Modell, J.W., Blat, I.C., Wrobel, M.J., Lerner, J., Brunet, J.P., Subramanian, A., Ross, K.N., et al. (2006). The

Connectivity Map: using gene-expression signatures to connect small molecules, genes, and disease. Science *313*, 1929–1935.

Lee, D.H., and Goldberg, A.L. (1998). Proteasome inhibitors: valuable new tools for cell biologists. Trends Cell Biol. *8*, 397–403.

Leung, D., Hardouin, C., Boger, D.L., and Cravatt, B.F. (2003). Discovering potent and selective reversible inhibitors of enzymes in complex proteomes. Nat. Biotechnol. *21*, 687–691.

Lin, C.M., and Hamel, E. (1981). Effects of inhibitors of tubulin polymerization on GTP hydrolysis. J. Biol. Chem. *256*, 9242–9245.

Liu, L.F. (1989). DNA topoisomerase poisons as antitumor drugs. Annu. Rev. Biochem. *58*, 351–375.

MacDonald, M.L., Lamerdin, J., Owens, S., Keon, B.H., Bilter, G.K., Shang, Z., Huang, Z., Yu, H., Dias, J., Minami, T., et al. (2006). Identifying off-target effects and hidden phenotypes of drugs in human cells. Nat. Chem. Biol. *2*, 329–337.

Maloney, A., Clarke, P.A., Naaby-Hansen, S., Stein, R., Koopman, J.O., Akpan, A., Yang, A., Zvelebil, M., Cramer, R., Stimson, L., et al. (2007). Gene and protein expression profiling of human ovarian cancer cells treated with the heat shock protein 90 inhibitor 17-allylamino-17-demethoxygeldanamycin. Cancer Res. *67*, 3239–3253.

McCollum, A.K., Teneyck, C.J., Sauer, B.M., Toft, D.O., and Erlichman, C. (2006). Up-regulation of heat shock protein 27 induces resistance to 17-allylamino-demethoxygeldanamycin through a glutathione-mediated mechanism. Cancer Res. *66*, 10967–10975.

Nowakowski, G.S., McCollum, A.K., Ames, M.M., Mandrekar, S.J., Reid, J.M., Adjei, A.A., Toft, D.O., Safgren, S.L., and Erlichman, C. (2006). A phase I trial of twice-weekly 17-allylamino-demethoxy-geldanamycin in patients with advanced cancer. Clin. Cancer Res. *12*, 6087–6093.

Nozawa, K., Tsuda, M., Ishiyama, H., Sasaki, T., Tsuruo, T., and Kobayashi, J. (2006). Absolute stereochemistry and antitumor activity of iejimalides. Bioorg. Med. Chem. *14*, 1063–1067.

Obrig, T.G., Culp, W.J., McKeehan, W.L., and Hardesty, B. (1971). The mechanism by which cycloheximide and related glutarimide antibiotics inhibit peptide synthesis on reticulocyte ribosomes. J. Biol. Chem. *246*, 174–181.

Parcellier, A., Schmitt, E., Gurbuxani, S., Seigneurin-Berny, D., Pance, A., Chantôme, A., Plenchette, S., Khochbin, S., Solary, E., and Garrido, C. (2003). HSP27 is a ubiquitin-binding protein involved in I-κBα proteasomal degradation. Mol. Cell. Biol. *23*, 5790–5802.

Parcellier, A., Brunet, M., Schmitt, E., Col, E., Didelot, C., Hammann, A., Nakayama, K., Nakayama, K.I., Khochbin, S., Solary, E., and Garrido, C. (2006). HSP27 favors ubiquitination and proteasomal degradation of p27Kip1 and helps S-phase re-entry in stressed cells. FASEB J. *20*, 1179–1181.

Parnaik, V.K. (2008). Role of nuclear lamins in nuclear organization, cellular signaling, and inherited diseases. Int. Rev. Cell Mol. Biol. *266*, 157–206.

Rai, S.S., and Wolff, J. (1998). Localization of critical histidyl residues required for vinblastine-induced tubulin polymerization and for microtubule assembly. J. Biol. Chem. *273*, 31131–31137.

Roca, J., Ishida, R., Berger, J.M., Andoh, T., and Wang, J.C. (1994). Antitumor bisdioxopiperazines inhibit yeast DNA topoisomerase II by trapping the enzyme in the form of a closed protein clamp. Proc. Natl. Acad. Sci. USA *91*, 1781–1785.

Rüegg, U.T., and Burgess, G.M. (1989). Staurosporine, K-252 and UCN-01: potent but nonspecific inhibitors of protein kinases. Trends Pharmacol. Sci. *10*, 218–220.

Saldanha, A.J. (2004). Java Treeview—extensible visualization of microarray data. Bioinformatics *20*, 3246–3248.

Sato, S., Kwon, Y., Kamisuki, S., Srivastava, N., Mao, Q., Kawazoe, Y., and Uesugi, M. (2007). Polyproline-rod approach to isolating protein targets of bioactive small molecules: isolation of a new target of indomethacin. J. Am. Chem. Soc. *129*, 873–880.

Schulte, T.W., Akinaga, S., Soga, S., Sullivan, W., Stensgard, B., Toft, D., and Neckers, L.M. (1998). Antibiotic radicicol binds to the N-terminal domain of Hsp90 and shares important biologic activities with geldanamycin. Cell Stress Chaperones *3*, 100–108.

Sheskin, D.J. (2000). Handbook of Parametric and Nonparametric Statistical Procedures, Second Edition (Boca Raton, FL: Chapman & Hall/CRC).

Sobell, H.M. (1985). Actinomycin and DNA transcription. Proc. Natl. Acad. Sci. USA *82*, 5328–5331.

Takatsuki, A., Arima, K., and Tamura, G. (1971). Tunicamycin, a new antibiotic. I. Isolation and characterization of tunicamycin. J. Antibiot. (Tokyo) *24*, 215–223.

Tanabe, K., Ikegami, Y., Ishida, R., and Andoh, T. (1991). Inhibition of topoisomerase II by antitumor agents bis(2,6-dioxopiperazine) derivatives. Cancer Res. *51*, 4903–4908.

Teruya, T., Simizu, S., Kanoh, N., and Osada, H. (2005). Phoslactomycin targets cysteine-269 of the protein phosphatase 2A catalytic subunit in cells. FEBS Lett. *579*, 2463–2468.

Tomiki, T., Saito, T., Ueki, M., Konno, H., Asaoka, T., Suzuki, R., Uramoto, M., Kakeya, H., and Osada, H. (2006). RIKEN Natural Products Encyclopedia (RIKEN NPEdia), a chemical database of RIKEN Natural Products Depository (RIKEN NPDepo). J. Comput. Aided Chem. *7*, 157–162.

Towbin, H., Bair, K.W., DeCaprio, J.A., Eck, M.J., Kim, S., Kinder, F.R., Morollo, A., Mueller, D.R., Schindler, P., Song, H.K., et al. (2003). Proteomics-based target identification: bengamides as a new class of methionine aminopeptidase inhibitors. J. Biol. Chem. *278*, 52964–52971.

Van den Bergh, G., and Arckens, L. (2004). Fluorescent two-dimensional difference gel electrophoresis unveils the potential of gel-based proteomics. Curr. Opin. Biotechnol. *15*, 38–43.

Vlahos, C.J., Matter, W.F., Hui, K.Y., and Brown, R.F. (1994). A specific inhibitor of phosphatidylinositol 3-kinase, 2-(4-morpholinyl)-8-phenyl-4H-1-benzopyran-4-one (LY294002). J. Biol. Chem. *269*, 5241–5248.

Whitesell, L., Mimnaugh, E.G., De Costa, B., Myers, C.E., and Neckers, L.M. (1994). Inhibition of heat shock protein HSP90-pp60v-src heteroprotein complex formation by benzoquinone ansamycins: essential role for stress proteins in oncogenic transformation. Proc. Natl. Acad. Sci. USA *91*, 8324–8328.

Yaguchi, S., Fukui, Y., Koshimizu, I., Yoshimi, H., Matsuno, T., Gouda, H., Hirono, S., Yamazaki, K., and Yamori, T. (2006). Antitumor activity of ZSTK474, a new phosphatidylinositol 3-kinase inhibitor. J. Natl. Cancer Inst. *98*, 545–556.